RSC Advances

PAPER

View Article Online
View Journal | View Issue

Check for updates

Cite this: *RSC Adv.*, 2020, **10**, 10740

Comparing chemical composition and lignin structure of *Miscanthus x giganteus* and *Miscanthus nagara* harvested in autumn and spring and separated into stems and leaves†

Michel Bergs,[ab] Xuan Tung Do,[a] Jessica Rumpf,[a] Peter Kusch,[a] Yulia Monakhova,[bc] Christopher Konow,[d] Georg Völkering,[e] Ralf Pude[ef] and Margit Schulze *[a]

Miscanthus crops possess very attractive properties such as high photosynthesis yield and carbon fixation rate. Because of these properties, it is currently considered for use in second-generation biorefineries. Here we analyze the differences in chemical composition between *M. x giganteus*, a commonly studied *Miscanthus* genotype, and *M. nagara*, which is relatively understudied but has useful properties such as increased frost resistance and higher stem stability. Samples of *M. x giganteus* (Gig35) and *M. nagara* (NagG10) have been separated by plant portion (leaves and stems) in order to isolate the corresponding lignins. The organosolv process was used for biomass pulping (80% ethanol solution, 170 °C, 15 bar). Biomass composition and lignin structure analysis were performed using composition analysis, Fourier-transform infrared (FTIR), ultraviolet-visible (UV-Vis) and nuclear magnetic resonance (NMR) spectroscopy, thermogravimetric analysis (TGA), size exclusion chromatography (SEC) and pyrolysis gas-chromatography/mass spectrometry (Py-GC/MS) to determine the 3D structure of the isolated lignins, monolignol ratio and most abundant linkages depending on genotype and harvesting season. SEC data showed significant differences in the molecular weight and polydispersity indices for stem *versus* leaf-derived lignins. Py-GC/MS and hetero-nuclear single quantum correlation (HSQC) NMR revealed different monolignol compositions for the two genotypes (Gig35, NagG10). The monolignol ratio is slightly influenced by the time of harvest: stem-derived lignins of *M. nagara* showed increasing H and decreasing G unit content over the studied harvesting period (December–April).

Received 16th December 2019
Accepted 9th March 2020

DOI: 10.1039/c9ra10576j

rsc.li/rsc-advances

Open Access Article. Published on 13 March 2020. Downloaded on 8/8/2024 5:01:17 AM.
This article is licensed under a Creative Commons Attribution-NonCommercial 3.0 Unported Licence.

1. Introduction

Low-input crops such as *Miscanthus* are currently studied as potential lignocellulose feedstock (LCF) for second-generation biorefineries,[1–5] as they possess a number of advantages over other industrial crops. Most importantly, *Miscanthus* belongs to the class of C4 plants, which binds four carbon atoms during oxaloacetic acid formation, as opposed to C3 plants, which only bind three carbon atoms during phosphoenolpyruvate formation.[6] *Miscanthus* crops are able to fix a higher amount of terrestrial carbon dioxide.

In addition, *Miscanthus* shows high photosynthesis yields, requires low amounts of fertilizer and has a high water use efficiency.[7–10] Like other perennial bioenergy crops such as short rotation coppice, *Miscanthus* was recently considered as an eligible ecological focus area within the European agricultural policy.[11] Potential applications of *Miscanthus* plants include renewable energy as well as the production of fuel and chemicals.[12–14] Recent studies include the investigation of cascade utilization of *Miscanthus* crops analogous to procedures reported for fruits.[15]

In difference to wood, grass-derived lignins show a significant amount of H units which is interesting for future applications. In literature, various groups reported specific lignin depolymerization procedures to isolate H-derived fragments.[16] Lignins isolated from grass and wood-based LCF using different pre-treatments and/or depolymerization procedures are

[a]*Department of Natural Sciences, Bonn-Rhein-Sieg University of Applied Sciences, von-Liebig-Straße 20, D-53359 Rheinbach, Germany. E-mail: margit.schulze@h-brs.de*
[b]*Spectral Service AG, Emil-Hoffmann-Strasse 33, D-50996 Köln, Germany*
[c]*Institute of Chemistry, Saratov State University, Astrakhanskaya Street 83, 410012 Saratov, Russia*
[d]*Department of Chemistry, Brandeis University, MS 015, 415 South Street, Waltham, Massachusetts, USA*
[e]*Institute of Crop Science and Resource Conservation, Faculty of Agriculture, University of Bonn, Klein-Altendorf 2, D-53359 Rheinbach, Germany*
[f]*Field Lab Campus Klein-Altendorf, Faculty of Agriculture, University of Bonn, Campus Klein-Altendorf 1, D-53359 Rheinbach, Germany*

† Electronic supplementary information (ESI) available. See DOI: 10.1039/c9ra10576j

This journal is © The Royal Society of Chemistry 2020

Open Access Article. Published on 13 March 2020. Downloaded on 8/8/2024 5:01:17 AM.
This article is licensed under a Creative Commons Attribution-NonCommercial 3.0 Unported Licence.

currently investigated for a broad variety of applications including lignin-based fuels, chemicals and polymer composites.[17,18] As a polyphenolic substance, lignin gained rising interest as substitute for fossil-based diols/polyols in polyurethane synthesis.[19–23] However, valorization of extracted lignin is still restricted to a few commercial products, mainly due to missing procedures for fast and reliable analysis of the highly complex 3D structure consisting of three randomly cross-linked monolignol units *p*-hydroxyphenyl (H), guaiacyl (G) and syringyl (S) (Fig. 1).

Cell wall composition and lignin contents of various *Miscanthus* genotypes including *M. x giganteus* and *M. sinensis* have intensively been investigated.[24–26] Fifteen *Miscanthus* genotypes (*e.g. M. sinensis*, *M. sacchariflorus*, *M. x giganteus*) harvested between November and April over a period of five years have been analyzed regarding their composition (ash, silicon, nitrogen, potassium, phosphorous, calcium, chlorine, and sulfur content). Compared to switchgrass and reed canary grass, *Miscanthus* genotypes showed significantly lower ash contents (1.6–4.0%, compared to 1.9–11.5%). In contrast to harvesting season, weather and/or ageing only slightly affected the crop composition.[27] Da Costa *et al.* reported a comprehensive study including 25 different *Miscanthus* genotypes (*M. x giganteus*, *M. sacchariflorus*, M. *sinensis* and hybrids of *M. sinensis*/*M. sacchariflorus*) separated by plant portions (stem, leaf). Mid-infrared spectroscopy was combined with chemometric analysis (*e.g.* principal component analysis, PCA) for quantification of the cell-wall composition, in particular structural carbohydrates. Results showed that the cell wall composition is a function of the tissue type: structural polysaccharides mainly cause differences in compositional variability for stem and leaf tissue. Therefore, the recalcitrance of stem and leaf might be determined by the carbohydrate composition.[28] In another very recent study, the authors presented a cell wall analysis to gain a deeper understanding of the cell wall recalcitrance including a huge number of genotypes of two main species: *M. sinensis* and *M. sacchariflorus* (and the hybrid *M. x giganteus*), separated into stems and leaves. Based on the results, future exploitation of *Miscanthus* should be directed to "specialized cultivars".[29]

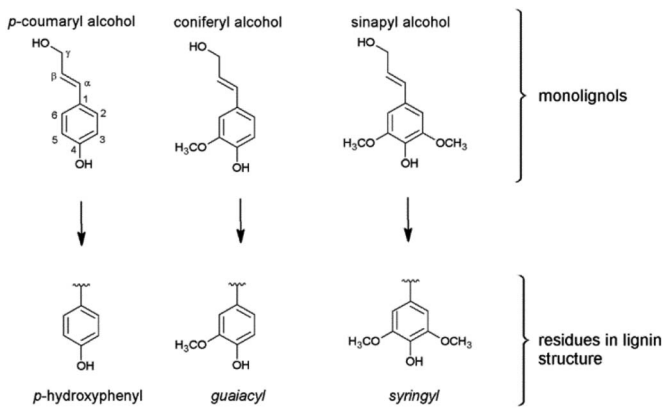

Fig. 1 The three monolignols and their corresponding structure units *p*-hydroxyphenyl (H), guaiacyl (G) and syringyl (S) of the lignin polymer.

Besides cell wall composition analysis, lignins have been isolated from *Miscanthus* plants and analyzed regarding their detailed 3D structure. Focus of most studies is the influence of the pre-treatment methods and corresponding parameters (*e.g.* temperature, pressure, solvent, catalyst) on the resulting lignin structure. In a comprehensive review, molecular weights and polydispersities and their dependencies on pre-treatment conditions are reported for a broad variety of lignins isolated from various biomasses (soft/hard wood, grasses) *via* different techniques (kraft, organosolv and others).[30]

El Hage *et al.* found correlations between the *Miscanthus*-derived lignin structure and the organosolv pre-treatment process parameters (temperature, sulfuric acid and ethanol concentration).[31,32] In another study, they confirmed the influence of process parameters on the resulting phenolic and aliphatic hydroxyl content, resulting in different lignin antioxidant activity.[33] Bauer *et al.* investigated a variety of lignins isolated from *Miscanthus x giganteus* using the organosolv process under reflux condition (using ethanol, acetone, dioxane). The increase of ethanol concentration resulted in a decreased carbohydrate content in the extracted lignin. Changes in monolignol ratio could be correlated with the biomass source.[34] In another approach, *M. x giganteus* lignins isolated *via* formosolv, organosolv, and cellulolytic enzyme treatments have been evaluated. Degradation was applied (acidic hydrolysis, reductive cleavage and thioacidolysis). According to 2D NMR results, β-O-4 linkages (82%) and acylated structures were the most dominant linkages. Highest purity (lowest carbohydrate content) has been achieved using the alkaline organosolv treatment.[35] Chan *et al.* reported the catalytic depolymerization of *M. x giganteus* using a vanadium catalyst for the organosolv process. Results showed significant differences in the reactivity of the lignin towards the catalyst and a selective cleavage of β-O-4′ linkages.[36] Luo *et al.* used a nickel catalyst for the depolymerization of *Miscanthus*-derived lignins into soluble fractions.[37] Enzymatic depolymerization of *Miscanthus* biomass has been studied mainly for bioethanol production[38] using wood rot fungi,[39] *Lentinula edodes*[40] or thermotolerant *Saccharomyces cerevisiae*,[41] which showed particularly significant depolymerization activity. Timilsena *et al.* used 2-naphthol and enzymatic hydrolysis for lignin isolation and studied the influence on the delignification of various crops including palm, typha grass and *M. x giganteus*.[42] Villaverde and Vanderghem compared lignins isolated from *M x giganteus* also using different pre-treatment methods, *e.g.* formic and acetic acid[43,44] and ammonia.[45]

Within the last decade, various ionic liquids have been studied for rapid pre-treatment of *Miscanthus* biomass, *e.g.* triethyl ammonium hydrogen sulfate resulting in specific correlation of treatment conditions and lignin structure.[46] According to Brandt *et al.*, ionic liquids preferably split the lignin–hemicellulose linkages, glycosidic, ester and β-O-4 ether bonds accompanied by a solubilization of the resulting lignin fragments. Increasing the pre-treatment time to 12 hours, repolymerization was observed. Furthermore, pre-treatment using ionic liquids could result in condensation reactions replacing aromatic C–H by C–C bonds.[47]

Open Access Article. Published on 13 March 2020. Downloaded on 8/8/2024 5:01:17 AM. This article is licensed under a Creative Commons Attribution-NonCommercial 3.0 Unported Licence.

Groenewold *et al.* specified the monolignol ratio of 34 *M. x giganteus* samples using both HSQC NMR and quantitative pyrolysis two-dimensional gas chromatography mass spectrometry method and compared both methods in detail.[48] This quantitative Py/GCxGC/MS is useful to describe thermal processing, but not appropriate to discover quantitative biomass composition. Compared to results obtained from HSQC NMR, Py/GCxGC/MS resulted in significantly lower values for S/G units *versus* much higher amount of H (4-vinylphenol).[48]

Harvesting effects on cell wall composition and saccharification of *M. x giganteus* have been investigated by several groups.[49–53] Huyen *et al.* reported that late harvesting correlates with increasing amounts of phenolic acids linked *via* ester bonds. Similar digestibilities have been observed for two harvesting times in case of enzymatic pre-treatment (using cellulases, β-glucosidase and xylanase).[53]

However, compared to *M. x giganteus*, little data is available for *M. nagara*, an interspecies hybrid of Japanese *M. sacchariflorus* and European *M. sinensis*, cultivated for example in Germany.[54] Characteristics of *M. nagara* are high stability due to strong stems, late mature, fast rhizome formation, good frost tolerance and a lower leaf loss during winter compared to *M. x. giganteus*. Published studies on *M. nagara* focus particularly the winter cold-tolerance thresholds, cultivation conditions and corresponding yields.[28,55–60] So far, these studies did not include structural details of lignins isolated from *M. nagara* cultivated in Europe.

In this study, twelve *M. x giganteus* (Gig35) and *M. nagara* (NagG10) samples (separated into stem and leaf) are analyzed for a side-by-side comparison regarding their chemical composition and lignin structure. Besides genotype and plant portion differences, the influence of the harvesting time (September, December, April) on the lignin chemical composition, most abundant linkages and G/H/S ratio is investigated.

2. Materials and methods

2.1 *Miscanthus* field trial

The crops presented in this study are cultivated at the Campus Klein-Altendorf (field lab of the Agricultural Faculty of the University of Bonn, Rheinbach, Germany).[8,9,61] The field stand was established in 2012. The replicates were obtained from field plots (each trial had four repetitions). Genotypes used in this study are *M. x giganteus* (cultivars 35, named as Gig35) and *M. nagara*, a hybrid of *M. sinensis* and *M. sacchariflorus* (NagG10). Samples were harvested in December 2014, April 2015, and September 2015. Stem material was taken from six different planting sites in the core parcel of the trial parcel (10 shoots). To investigate single plant portions (stem *versus* leaf), stem and leaves were separated at the ligule. All samples were dried before milling (24 hours, 105 °C).

2.2 Lignin isolation *via* organosolv pulping

All *Miscanthus* samples were milled (Pulverisette 6, Fritsch, Germany) and sieved (Modell AS 200 basic, Retsch, Germany) to a particle size <0.5 mm. The organosolv pulping was then performed according to recently published procedures.[62–64] 50 g *Miscanthus* biomass was mixed with 400 mL of an 80% (v/v) ethanol solution in a Parr reactor (1.0 L stainless steel) with a 4848 Reactor Controller and heated to 170 °C under continuous stirring. The maximum temperature was held for 90 minutes. After cooling down the autoclave, the biomass was filtered and washed with an 80% (v/v) ethanol solution (50 mL) for five times. The filter cake was rejected and the filtrate was mixed with approx. three volumes of water and 10 mL hydrochloric acid (HCl, 37%) to precipitate the organosolv lignin. The precipitate was separated by centrifugation (Hettich Rotina 420, 3500 rpm, 5 minutes), washed three times with dist. water and freeze-dried for 72 h.

2.3 Composition analysis including lignin, ash and sugar content

The chemical composition (%, w/w) of *Miscanthus* genotypes was determined according to the Laboratory Analytical Procedures (LAP) published by the National Renewable Energy Laboratory (NREL).[65] These measurements were performed at the Biopos Institute in Teltow-Seehof, Germany. In short, structural carbohydrates and lignin in biomass were determined following NREL/TP-510-42618, water and ethanol soluble extractives in biomass according to NREL/TP-510-42619, total solids in biomass according to NREL/TP-510-42621 and ash content according to NREL/TP-510-42622.[66–69]

2.4 Size exclusion chromatography (SEC)

SEC measurements were performed using a PSS SECcurity^2 GPC System (Mainz, Germany) with two PSS SDV 8 × 300 mm Linear M 5μ columns and pre-column with UV detection (280 nm). Tetrahydrofuran (THF) was used as eluent with a flow rate of 1.0 mL min^{-1}, an injection volume of 60 μL and a total run time of 30 minutes. Samples were dissolved in THF (10 mg mL^{-1}) with gentle stirring and filtered through a 0.2 μm PTFE filter prior to analysis. For calibration, polystyrene was used in a calibration range of 376–2 570 000 g mol^{-1}.

2.5 Ultraviolet-visible (UV-Vis) spectroscopy

UV-Vis spectra were recorded on a PerkinElmer Lambda 35 with UV WinLab 6.0.2.0723. Lignins were dissolved in THF (0.5 mg mL^{-1}) and measured at room temperature in a range of 200–400 nm against THF.

2.6 Fourier-transform infrared (FT-IR) spectroscopy

FT-IR spectra were recorded with a Jasco FT/IR 410 spectrometer with Spectra Manager Version 1.54.03 over 8 scans with a resolution of 4 cm^{-1} in a wave number range of 4000–700 cm^{-1}. A 300 mg KBr disk containing 2 mg of finely grounded sample was used.

2.7 Nuclear magnetic resonance (NMR) spectroscopy

Measurements were performed on an NMR spectrometer Avance III 600 (Bruker, Karlsruhe, Germany) to obtain 2D HSQC NMR spectra with 4 scans and 16 prior dummy scans (using *ca.* 100 mg of lignin solved in 1 mL deuterated d-DMSO). Data of

Open Access Article. Published on 13 March 2020. Downloaded on 8/8/2024 5:01:17 AM.
This article is licensed under a Creative Commons Attribution-NonCommercial 3.0 Unported Licence.

4000 points were recorded with 7211 Hz spectral width, 2050 receiver gain and 0.28 s total acquisition time. O1 was set to 5 ppm for ^{1}H and 80 ppm for ^{13}C.

2.8 Thermogravimetric analysis (TGA)

TGA measurements were performed with approx. 10 mg of lignin using a TGA 209 F1 (Netzsch, Selb, Germany) with a heating rate of 20 °C min^{-1} under nitrogen atmosphere from ambient to 900 °C. Synthetic air was used for an isothermic combustion at 900 °C.

2.9 Pyrolysis-gas chromatography/mass spectrometry (Py-GC/MS)

For Py-GC/MS measurements, a combination of an EGA/PY-3030D multi-shot pyrolyzer (Frontier Lab, Fukushima, Japan), two GC 2010 Plus gas chromatographs with two fused silica capillary columns (Ultra Alloy columns: UA5-30M-0.25F and UACW-20M-0.25F; length of 30 m and 20 m respectively, inside diameter 0.25 mm, film thickness 0.25 μm) and a GCMS-QP2010 Ultra mass spectrometer (Shimadzu, Kyoto, Japan) was used. For the measurement the Shimadzu software MDGC Analysis GC solution 2.41.00. SU1 was used, evaluation was performed with Shimadzu GC/MS solution 2.72.[70] The lignin sample (0.5 mg) was placed in a stainless-steel pyrolysis crucible (PY1-EC50F) and pyrolyzed at 550 °C. For GC separation, a temperature program (1 min at 75 °C, then 280 °C for 25 min with a heating rate of 7 °C min^{-1}) was used for the first column, the second one was isothermally tempered at 200 °C. The carrier gas used was helium 4.0 (Westfalen AG, Münster, Germany). For the MS detection, ionization was carried out *via* electron impact (EI) at 70 eV. Ions were detected by their mass/charge ratio (*m*/*z*); the measuring range was 35–740 u.

3. Results and discussion

3.1 *Miscanthus* crop compositional analysis

Both genotypes, *M. x giganteus* (Gig35) and *M. nagara* (NagG10), show comparable plant growth: from September to December, the leaf-to-stem ratio increases to a maximum at the end of the year. Then, as the crops start to lose most of their leaves the leaf-to-stem-ratio reaches its minimum (Fig. 2).

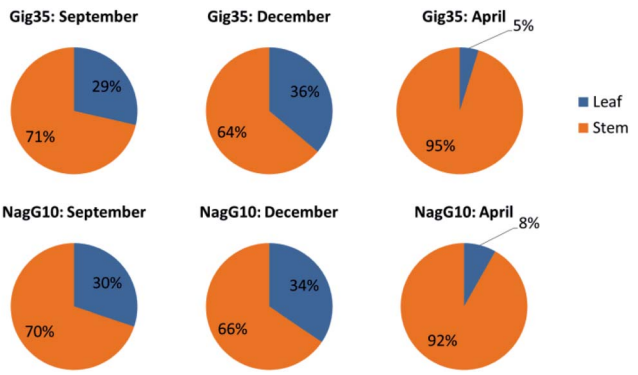

Fig. 2 Leaf *versus* stem content of *M. x giganteus* (Gig35) (top row) and *M. nagara* (NagG10) (bottom row) harvested in September, December and April.

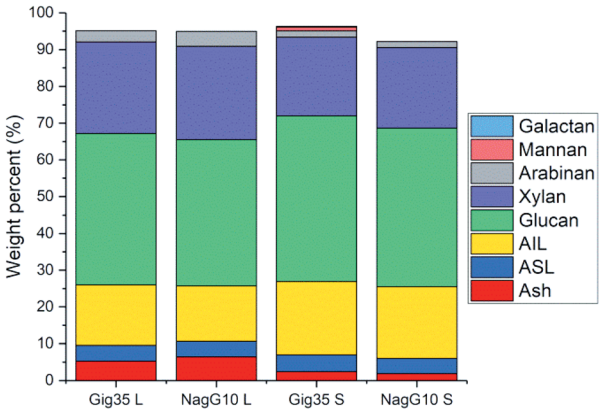

Fig. 3 Compositional analysis data (according to NREL protocol) of *M. x giganteus* (Gig35) and *M. nagara* (NagG10) separated into leaf (L) and stem (S), all harvested in April 2015. AIL: acid-insoluble lignin. ASL: acid-soluble lignin. Ash description: total ash (in %). Further details see Table S1.†

Table 1 Compositional analysis data (according to NREL protocol) of *Miscanthus* genotypes (Gig35, Nag10) harvested in April 2015. AIL: acid-insoluble lignin. ASL: acid-soluble lignin. AIR: acid-insoluble residuals. AIA: acid-insoluble ash. Errors are given as standard deviation of triplicates

Portion	Leaf		Stem	
Genotype	Gig35	NagG10	Gig35	NagG10
Galactan (%)	n.d.	n.d.	0.2 ± 0.4	n.d.
Mannan (%)	n.d.	n.d.	1.0 ± 1.4	n.d.
Arabinan (%)	3.1 ± 0.3	4.1 ± 0.1	1.7 ± 0.3	1.7 ± 1.5
Xylan (%)	24.9 ± 0.5	25.4 ± 1	21.4 ± 0	21.9 ± 0.5
Glucan (%)	41.2 ± 0.9	39.8 ± 2.2	45.1 ± 0.4	43.1 ± 1.3
AIL (%)	16.4 ± 0.8	15.1 ± 0.3	20 ± 0.1	19.5 ± 0.1
ASL (%)	4.3 ± 0	4.2 ± 0	4.6 ± 0.1	4.2 ± 0.1
AIR (%)	17.1 ± 1.0	16.5 ± 0.2	20.4 ± 0.1	19.9 ± 0.1
Total lignin (%)	22.9 ± 0.7	19.3 ± 0.3	24.6 ± 0.2	23.6 ± 0.1
AIA (%)	0.7 ± 0.1	1.4 ± 0.1	0.5 ± 0.02	0.5 ± 0.1
Total ash (%)	5.2	6.4	2.4	1.9
Dry matter (%)	91.2	91.4	92.2	93.0

As stated in the introduction, the leaf loss during winter for *M. nagara* is less intensive compared to other types such as *M. x giganteus*.[54–60] Biomass composition including ash, carbohydrate and lignin content was determined for stem and leaf samples of both genotypes (Gig35 and NagG10) harvested in April (Fig. 3 and Table 1).

Stems show higher lignin content than leaves for both genotypes (Fig. 3 and Table 1): *M. x. giganteus* leaves (Gig35L) showed 16.43 ± 0.78% acid-insoluble lignin (AIL) *versus* 19.92 ± 0.10% for stems (Gig35S); *M. nagara* leaves (NagG10L) showed 15.10 ± 0.31% AIL *versus* 19.49 ± 0.08% for stems (NagG10S). These results are in accordance with previously reported data for two other *M. x giganteus* genotypes.[61] Other literature studies focusing on the chemical composition of specific plant portions

Open Access Article. Published on 13 March 2020. Downloaded on 8/8/2024 5:01:17 AM.
This article is licensed under a Creative Commons Attribution-NonCommercial 3.0 Unported Licence.

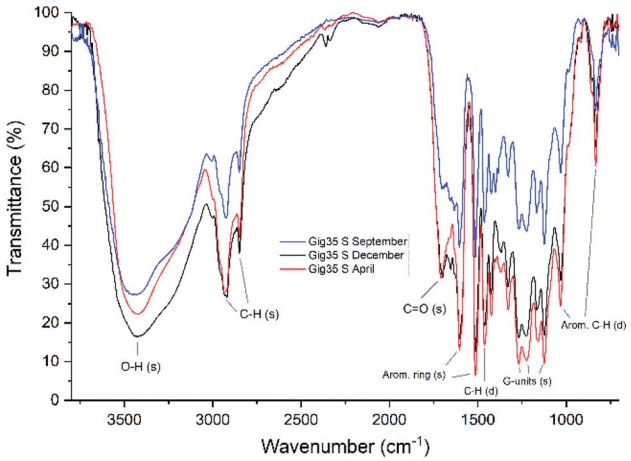

Fig. 4 FTIR spectra of stem-derived lignins obtained from *M. x giganteus* (Gig35S), harvested in September, December and April.

reported lignin contents varying between 19–25% for *M. x. giganteus* Soerensen, Cha.[38,41]

The lowest lignin content was observed for leaves in NagG10, whereas stems of Gig35 showed highest lignin content. Significant differences in cell-wall composition of *Miscanthus* stem and leaf samples were also observed by other groups: compared to leaves, increased lignin contents were found in stems.[31,32] For both genotypes the glucan (cellulose) content was only slightly higher in stems (statistical significance has to be confirmed in ongoing measurements). There is about 2% more cellulose overall in Gig35 than NagG10. Hemicellulose has been determined to mostly consist of xylan with minor contents of arabinan, which was also observed in previous studies for *M. x giganteus* genotypes.[13,14,61] The content of both hemicellulose monomers were higher in leaves than in stems.

3.2 Structural differences of isolated lignins

FTIR data obtained for both *M. x giganteus* and *M. nagara* (Gig35 and NagG10) are in good accordance with reported data

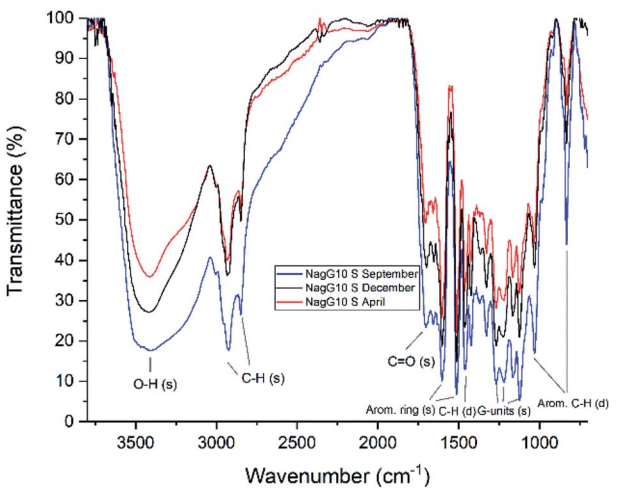

Fig. 5 FTIR spectra of stem-derived lignins obtained from *M. nagara* (NagG10), harvested in September, December and April.

for other *Miscanthus*-derived lignins.[31–34,47,61] Leaf-derived lignins of both genotypes (Gig35 and NagG10) showed comparable development from September to April. In detail, the C=O stretching signal (1708 cm^{-1}) is very weak in September and increases until April for both Gig35 and NagG10. In contrast, the intensity of this signal decreases in stems (Fig. 4 and 5, see also ESI Fig. S1† for signal numbering and Table S1† for signal assignment).

From September to April, the signal intensity of the anti-symmetric deformation C–H in methoxy groups at 1424 cm^{-1} and the aromatic skeletal C–O stretching band at 1331 cm^{-1} increase in stems and leaves, representing the S unit formation in lignin biosynthesis (see Fig. 1).

In general, information obtained by FTIR spectroscopy is limited due to strong signal overlap. Here, multivariate data analysis is a very helpful tool to "extract" details that are not available using conventional univariate analysis as shown also by other groups for lignins of different origin and pre-treatment method.[71,72] In a previous study, we also used chemometric processing of infrared data to specify differences of lignins obtained from six different *Miscanthus* genotypes including *M. nagara* (NagG10) and *M. x giganteus* (Gig35) separated by plant portions: stem *versus* leaf-derived lignins could be differentiated by their aromatic in-plane deformation signals at 1160 cm^{-1} corresponding to the monolignol substitution pattern.[61]

3.3 Ultraviolet-visible absorption of isolated lignins

Due to a strong signal overlap of absorption bands of the manifold functional groups in lignin, UV-Vis is only used for purity control and quantitative analysis rather than compound identification, as shown for various biomasses (*e.g.* willow, aspen, softwood, canary grass and hemp).[73] For kraft lignins isolated from industrial black liquor, the UV absorbance is directly correlated to the purity level: at higher pH values for lignin isolation, a lower absorbance is observed due to the co-precipitation of degraded polysaccharides and/or lipids.[74] Furthermore, solvent extraction of kraft lignin results in four distinct absorption bands.[75]

UV-Vis spectra are shown in the ESI (Fig. S2–S5)† for stem- and leaf-derived samples of *M. x giganteus* (Gig35) and *M. nagara* (NagG10) harvested in September, December and April. Although all samples showed comparable spectra, there are some distinct differences: the plant development from September to April could be observed for both genotypes, more clearly for the leaf-derived lignins than those isolated from stems. In accordance to literature data for wood- and grass-based lignins,[76,77] at 280 nm a strong absorption band was observed corresponding to the π–π^* transition of the aromatic core. At higher wavelengths around 310 nm, fragments of enhanced conjugation were obtained (*e.g.* hydroxy cinnamoyl derivatives). As opposed to lignins isolated from whole plants (mixtures of stem and leaves), in leaf-derived lignins the amount of structural fragments of higher conjugation showed a clear increase from September to April (see ESI, Fig. S2 and S4†). This is in accordance with previously reported results for other *Miscanthus*-derived lignins.[61]

 This journal is © The Royal Society of Chemistry 2020

Open Access Article. Published on 13 March 2020. Downloaded on 8/8/2024 5:01:17 AM.
This article is licensed under a Creative Commons Attribution-NonCommercial 3.0 Unported Licence.

Table 2 TGA results including first and second mass loss (ML), residual mass (RM), and decomposition temperature (T_d) for two leaf-derived (Gig35L, NagG10L) and two stem-derived (Gig35S, NagG10S) *Miscanthus* lignins harvested in September, December and April

Sample	First ML (120 °C)	Second ML (350 °C)	RM	T_d
Gig35L Sept	1.4%	72%	26.6%	363.6 °C
Gig35L Dec	1.8%	74.1%	24.1%	363.8 °C
Gig35L April	0.4%	69.5%	30.1%	346.1 °C
NagG10L Sept	0.9%	78%	21.1%	353.7 °C
NagG10L Dec	1.7%	77.7%	20.5%	352.2 °C
NagG10L April	0.3%	68.7%	31%	357.3 °C
Gig35S Sept	3.6%	60.9%	35.4%	364.6 °C
Gig35S Dec	3.2%	64.2%	32.5%	385.5 °C
Gig35S April	2.3%	67.0%	30.7%	356.8 °C
NagG10S Sept	1.3%	64.2%	34.5%	381.3 °C
NagG10S Dec	1.7%	72.1%	26.2%	351.9 °C
NagG10S April	1.1%	67.2%	31.6%	362.7 °C

3.4 Thermal stability of isolated lignins

The thermal behavior of the lignins was determined using thermogravimetric analysis. In Table 2, the TGA data obtained in this study are summarized including temperature-dependent mass loss (ML), residual masses (RM) and decomposition temperatures (T_d) for leaf (Gig35L, NagG10L) and stem-separated samples (Gig35S, NagG10S).

In general, the first mass loss (measured after a few minutes at about 120 °C) can be assigned to the elimination of low molecular weight substances and moisture (carbon monoxide, carbon dioxide, water). The depolymerization of lignin occurs within a rather broad temperature range between 170–700 °C. The monolignol linkages show different thermal stabilities, with lower values for propanoid side chains degraded into methyl, ethyl, and vinyl guaiacol derivatives. Highest stabilities were assigned to C–C linkages.[78–80] In both, wood-derived kraft and *Miscanthus* lignins, the monolignol units are mainly connected by β-O-4 linkages resulting in comparable decomposition temperatures[74] as recently also shown for other *M. x giganteus* samples Bergs.[61] Regarding genotype, plant portion and/or harvesting time, no correlations could be specified for TGA data.

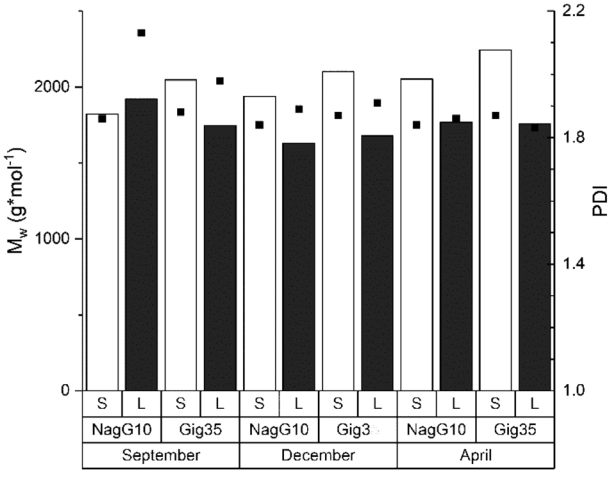

Fig. 6 Size exclusion chromatography results including the weight average molecular weight (MW, columns) and polydispersity index (PDI, squares) of lignins obtained from *M. x giganteus* and *M. nagara*, respectively, separated into leaves (Gig35 L, NagG10L) and stems (Gig35S, NagG10S). Further details see ESI Table S2.†

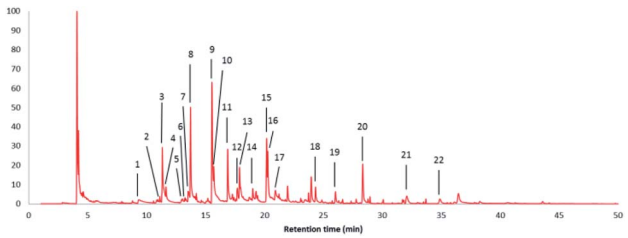

Fig. 7 Pyrolysis-GC/MS pyrogram of a stem-derived lignin obtained from *M. x giganteus* (Gig35S) harvested in April with peak picking for all aromatic fragments listed and assigned in Table 3.

3.5 Lignin molecular weight and polydispersity

The molecular weight is a fundamental characteristic influencing the biomass recalcitrance mainly depends on the biomass source (wood, grass *etc.*) and procedure used for lignin isolation (kraft, organosolv, ionic liquids *etc.*). As shown in previous studies for beech wood[81,82] and *Miscanthus*-derived lignins,[31–34,61] ethanol organosolv pre-treatment is an appropriate method to produce lignins of rather low molecular weight (MW) and narrow MW

Table 3 Pyrolysis-GC/MS fragments of the sample Gig35S (stem-derived *M. x giganteus*) harvested in April and assignment to H, G, and S units

Peak no.	Retention time (min)	Content (%)	Name	Assignment
1	9.338	2.29	Phenol	H
2	11.105	0.51	*o*-Cresol	H
3	11.325	9.99	Guaiacol	G
4	11.630	2.42	*p*-Cresol	H
5	12.942	0.36	2,6-Xylenol	H
6	13.248	0.15	2,4-Xylenol	H
7	13.518	2.25	4-Ethylphenol	H
8	13.720	10.60	Creosol	G
9	15.536	17.00	Coumaran	H
10	15.688	7.70	4-Ethylguaiacol	G
11	16.875	7.51	4-Hydroxy-2-methyl acetophenone	H
12	17.698	2.06	Eugenol	G
13	17.873	5.17	Syringol	S
14	19.000	1.14	*cis*-Isoeugenol	G
15	20.180	7.40	4-Methylsyringol	S
16	20.272	5.89	*trans*-Isoeugenol	G
17	20.914	2.65	Vanillin	G
18	24.321	2.10	4-Allylsyringol	S
19	26.019	1.69	4-Propenylsyringol isomer	S
20	28.335	6.61	4-Propenylsyringol isomer	S
21	32.066	2.25	Syringylaldehyde	S
22	34.875	1.23	Acetosyringone	S

Open Access Article. Published on 13 March 2020. Downloaded on 8/8/2024 5:01:17 AM.
This article is licensed under a Creative Commons Attribution-NonCommercial 3.0 Unported Licence.

distribution. Thus, the molecular weight and polydispersities determined for Gig35 and NagG10 are significantly lower compared to soft/hard wood-derived kraft lignins.

In general, polydispersities for technical wood-based kraft lignin vary between 2.6 to 6.5 (depending on pre-treatment conditions), whereas *Miscanthus*-lignins of different genotype showed polydispersities below 1.7.[30,82] Except for leaf-derived lignin of NagG10 harvested in September, the studied leaf-derived samples also possess polydispersities below 2 (Fig. 6 and ESI Table S2†).

Regarding the influence of harvesting season, an increase of the molecular weight was observed for stem-derived lignins of both genotypes during the harvesting cycle (from September to April). According to the literature, the polydispersity index (PDI) should slightly decrease until April as a result of the unfinished lignin biosynthesis: during the biosynthesis process, the three monolignol units are step-wise linked to each other thereby decreasing the number of fragments of lower molecular weight.[83,84] The obtained results for Gig35 and NagG10 samples showed no significant difference in MW and PDI for the harvesting period. To obtain a deeper insight, ongoing studies include diffusion ordered spectroscopy (DOSY) NMR as recently used by Montgomery *et al.*[85]

Table 4 Monolignol ratio (G, H, S) of lignins according to pyrolysis – GC/MS data of *M. x giganteus* (Gig35) and *M. nagara* (NagG10)

Sample	H (%)	G (%)	S (%)
Gig35L Sept	55	34	11
Gig35L Dec	54	41	5
Gig35L April	49	39	12
NagG10L Sept	61	30	9
NagG10L Dec	52	36	12
NagG10L April	41	46	13
Gig35S Sept	42	35	23
Gig35S Dec	46	41	13
Gig35S April	33	41	26
NagG10S Sept	45	32	23
NagG10S Dec	39	37	24
NagG10S April	35	40	25

3.6 Monolignol ratio and linkages due to pyrolysis GC/MS

Fig. 7 shows the pyrolysis-GC/MS pyrogram of a stem-derived lignin obtained from *M. x giganteus* (Gig35S) harvested in April with numbers for all aromatic fragments listed and assigned in Table 3.

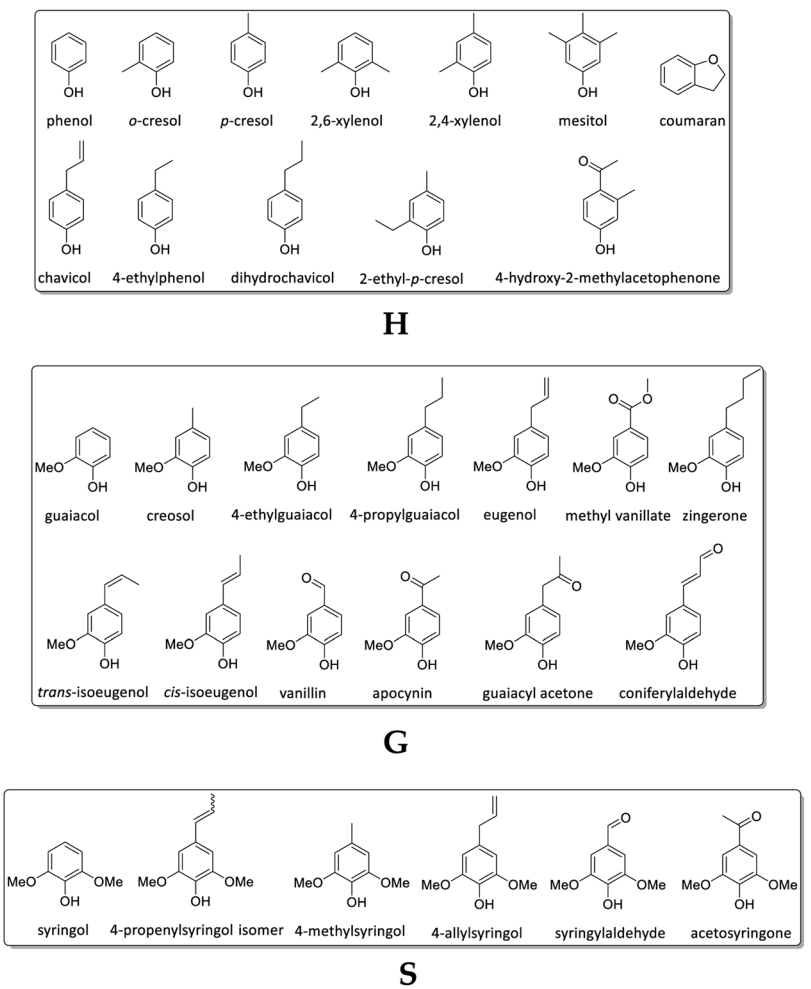

Fig. 8 Detected Py-GC/MS fragments attributed to the three subunits (G, H and S).

 This journal is © The Royal Society of Chemistry 2020

Open Access Article. Published on 13 March 2020. Downloaded on 8/8/2024 5:01:17 AM.
This article is licensed under a Creative Commons Attribution-NonCommercial 3.0 Unported Licence.

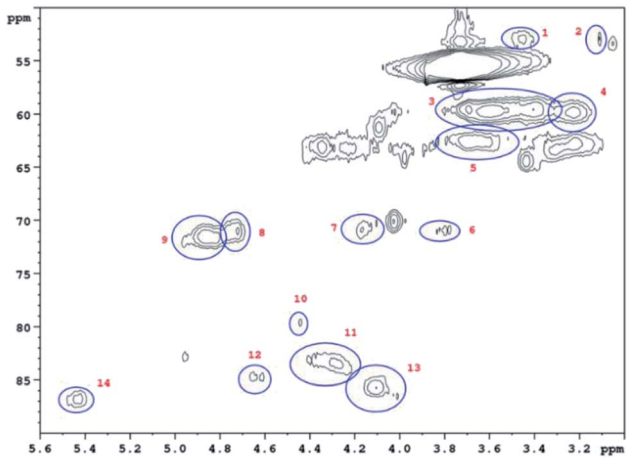

Fig. 9 Non-Aromatic HSQC region of a lignin obtained from *M. nagara* (NagG10, stem, April harvest). Numbers are listed and assigned in Table 5.

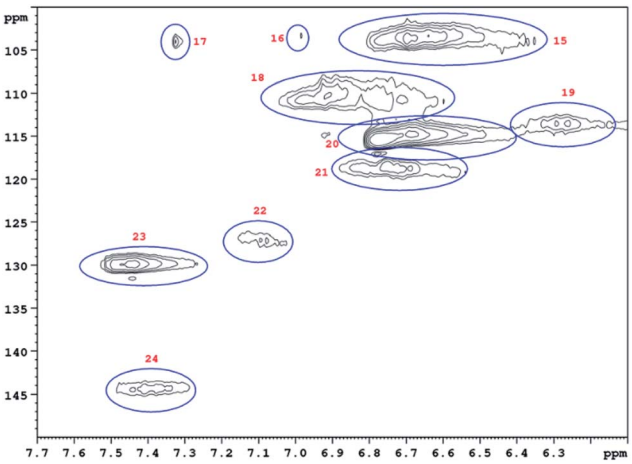

Fig. 10 Aromatic HSQC region of a lignin obtained from *M. nagara* (NagG10, stem, April harvest). Numbers are listed and assigned in Table 5.

In Fig. 8, the detected Py-GC/MS fragments are summarized and grouped by subunit (G, H, and S) to which they could be attributed.

Table 4 shows the monolignol ratio (G, H, S) of lignins according to pyrolysis – GC/MS data of *M. x giganteus* (Gig35) and *M. nagara* (NagG10).

The studies revealed a decreasing amount of H units in leaves (particularly in NagG10) and a simultaneous increase of G units in both genotypes over the harvesting period. In stem-derived lignins the H units were also decreasing, whereas G and S were increasing. In general, the signal assignment to monolignol units follows literature reports[86–89] (although no data are available yet for *M. nagara*, stem/leaf portions harvested at different times). As stated by Groenewold *et al.*, Py-GC/MS is useful to describe thermal processing, but not appropriate to discover quantitative biomass composition. Compared to results obtained from HSQC NMR, Py/GCxGC/MS resulted in

Table 5 HSQC 2D NMR data for a lignin isolated from *M. nagara* stems (NagG10S) harvested in April. HSQC 2D NMR spectra of the non-aromatic and aromatic region see ESI Fig. S6 and S7

No.	Integral (rel)	δ ^{1}H (ppm)	δ ^{13}C (ppm)	Name	Assignment
1	0.0190	3.45	52.88	B β	B
2	0.0254	3.06	53.34	C β	C
3	0.7089	3.56	59.66	A γ	A
4	0.1322	3.23	59.71	B γ	B
5	0.1932	3.68	62.73	A γ	A
6	0.0321	3.82	71.00	C γ	C
7	0.0441	4.17	70.76	C γ	C
8	0.0561	4.74	70.95	A α	A
9	0.1541	4.86	71.37	A α	A
10	0.0435	4.47	79.78	A β	A
11	0.1160	4.31	83.63	A β	A
12	0.0361	4.64	84.75	C α	C
13	0.1106	4.07	85.77	A β	A
14	0.0626	5.45	86.79	B α	B
15	0.7042	6.73	103.42	S 2/6	S
16	0.0411	6.99	103.24	S 2/6	S
17	0.0337	7.33	103.79	S 2/6	S
18	0.4662	6.96	109.88	G 2	G
19	0.1192	6.30	113.46	D β	D
20	1.0000	6.71	114.80	G 5	G
21	0.1827	6.79	118.61	G 6	G
22	0.1588	7.12	127.35	H 2/6	H
23	0.4032	7.48	129.07	H 2/6	H
24	0.1315	7.43	143.84	D α	D

significantly lower values for S/G units *versus* much higher amount of H (4-vinylphenol).[48]

3.7 Monolignol ratio and linkages due to HSQC NMR

HSQC 2D NMR spectra have been recorded showing the non-aromatic region and aromatic region (Fig. 9 and 10) of a lignin obtained from *M. nagara* stems (NagG10S) harvested in April. HSQC spectra of stem-derived *M. x giganteus* (Gig35) harvested in April are shown in ESI Fig. S6 and S7.† The numbered and assigned signals are listed in Table 5.

Table 6 summarizes the ratio of the monomer units (H, G, S) and of the most abundant linkages obtained from *M. x giganteus* (Gig35) and *M. nagara* (NagG10) stem and leaf-derived lignins harvested in September, December and April.

For leaf-derived lignins, results revealed a decrease of H and increase of G unit content from September to April, in particular for NagG10L. For the same harvesting period, stem-derived lignins showed a decrease of H and S, which was more clear for NagG10S compared to Gig35S. Beside monolignol ratio, the influence of the harvesting season on the number and nature of formed linkages (A: β-O-4 linkage, B: phenylcoumaran, C: resinol, D: unsaturated ester) has been investigated (Table 6 and Fig. 11).

In September a higher amount of β-aryl ether linkages (A) was observed in leaves compared to stems for both genotypes. Until April, theses linkages (A) significantly decrease to similar amounts (for both leaf and stem). Phenylcoumaran (B) and resinol (C) linkages were slightly increasing for leaves in both

Open Access Article. Published on 13 March 2020. Downloaded on 8/8/2024 5:01:17 AM.
This article is licensed under a Creative Commons Attribution-NonCommercial 3.0 Unported Licence.

Table 6 Ratio of the monomer units (H, G, S) and of the most abundant linkages in lignins obtained from *M. x giganteus* (Gig35) and *M. nagara* (NagG10) stem (S) and leaf (L)-derived, harvested in September, December and April. Corresponding structures are shown in Fig. 11

Sample	H (%)	G (%)	S (%)	A (β-aryl ether) (%)	B (phenylcoumaran) (%)	C (resinol) (%)	D (unsaturated ester) (%)
Gig35L Sept	28	52	20	73	9	5	13
Gig35L Dec	13	63	24	69	9	5	17
Gig35L April	18	61	21	60	10	8	22
NagG10L Sept	31	48	21	72	7	4	17
NagG10L Dec	20	57	23	59	8	5	28
NagG10L April	18	62	20	59	10	8	23
Gig35S Sept	19	53	28	58	8	7	27
Gig35S Dec	17	58	25	56	9	7	28
Gig35S April	18	56	26	56	9	7	28
NagG10S Sept	21	50	29	56	9	7	28
NagG10S Dec	16	56	28	57	9	6	28
NagG10S April	16	57	27	57	9	8	26

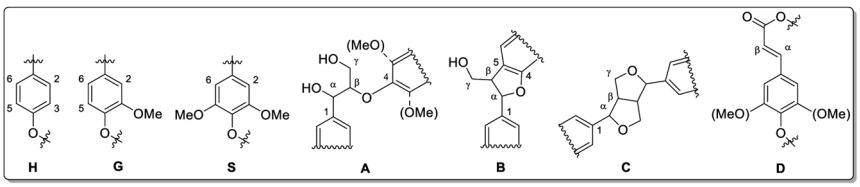

Fig. 11 Lignin structure elements for HSQC NMR signal assignment (A: β-O-4 linkage, B: phenylcoumaran, C: resinol, D: unsaturated ester). Reprinted from ref. 61 under open access license.

genotypes. In stem-derived lignins, C was unchanged. The amount of β-unsaturated esters (D) was increasing in leaves. Du *et al.* reported NMR data for *Miscanthus*-derived lignins obtained *via* hydrolase treatment and quantitative fractionation containing carbohydrate residuals and corresponding linkages.[90] The samples discussed in the present study did not show any of those linkages, confirming the high purity (in accordance with composition analysis data, see Section 3.1).

HSQC NMR data reported for lignocellulosic biomass separated into stem and leaf discuss the cell wall composition including lignin amount and polysaccharide-lignin-linkages.[34,46,47,61,90–92] Although NMR is a rather fast and easy method, the problem of signal overlap (even in 2D NMR) restricts quantitative data interpretation. Here, multivariate data processing (such as partial component analysis, linear discriminant analysis, factorial discriminant analysis and partial least squares-discriminant analysis) proved to be a useful tool for origin specification of complex structures such as lignocellulosic biomass, especially lignin.[71,72,93–99]

Moreover, Brandt *et al.* emphasized that quantification using HSQC is generally limited since pulse sequences are usually optimized for resolution and signal strength. In addition, signal relaxation might not be complete particularly for some slowly relaxing end groups. As mentioned before, Groenewold *et al.* compared the ratio of monolignol units obtained by quantitative Py-GCxGC-MS and HSQC NMR, respectively. In case of Py-GCxGC-MS, the amount of S-/G-units was lower and H was higher compared to data obtained by HSQC.[48] Both genotypes studied here also showed higher amounts of H units in Py-GC/MS compared to HSQC NMR.

4. Conclusions

Two different *Miscanthus* genotypes (*M. x giganteus* and *M. nagara*) harvested at three different times and separated into leaf and stem portions have been analyzed regarding their chemical composition. Lignins of both genotypes, isolated *via* ethanol organosolv pre-treatment, showed significantly lower polydispersities and thus higher homogeneity compared to technical kraft lignin emphasizing the promising potential of both, *Miscanthus* biomass and organosolv procedure, to be used for lignin recovery. Due to the better frost resistance and higher stem stability, *M. nagara* offers some advantages compared to *M. x giganteus*.

A side-by-side comparison of the two genotypes revealed only slight differences for the chemical composition and monolignol linkages depending on the harvesting month (September, December, April). Stem-derived lignins of *M. nagara* showed a decrease of H and increase of G units during the studied harvesting period. However, further studies are required since differences still remain between G/H/S ratio obtained by HSQC NMR *versus* Py-GC/MS as reported by other research groups.

Conflicts of interest

There are no conflicts to declare.

 This journal is © The Royal Society of Chemistry 2020

Open Access Article. Published on 13 March 2020. Downloaded on 8/8/2024 5:01:17 AM.
This article is licensed under a Creative Commons Attribution-NonCommercial 3.0 Unported Licence.

Acknowledgements

Funding was given by the BMBF program IngenieurNachwuchs (project LignoBau, 03FH013IX4) and BioSC project *Miscanthus* Cascade Utilization (NRW state ministry for research). M. B. and J. R. obtained a PhD scholarship by the Graduate Institute of Bonn-Rhein-Sieg University of Applied Sciences (GI HBRS). Y. M. acknowledges support from the Russian Science Foundation (project 18-73-10009).

References

1 The European Economic and Social Committee and the Committee of the Regions, *Communication from the Commission to the European Parliament, the Council*, The European Commission, Brussels, Belgium, 2018, Reference No. 11.10.2018 COM.
2 S. S. Hassan, G. A. Williams and A. K. Jaiswal, *Trends Biotechnol.*, 2019, **37**, 231.
3 S. Vanhamaki, K. Medkova, A. Malamakis, S. Kontogianni, E. Marisova, D. Huisman-Dellago and N. Moussiopoulos, *Int. J. Sustain. Dev. Plann.*, 2019, **14**, 31.
4 A. Alzagameem, M. Bergs, X.-T. Do, S. E. Klein, J. Rumpf, M. Larkins, Y. Monakhova, R. Pude and M. Schulze, *Appl. Sci.*, 2019, **9**, 2252.
5 K. Van Meerbeek, B. Muysa and M. Hermy, *Renewable Sustainable Energy Rev.*, 2019, **102**, 139.
6 E. A. Kellogg, *Curr. Biol.*, 2013, **23**, R594.
7 I. Lewandowski, J. Clifton-Brown, L. M. Trindade, *et al.*, *Front. Plant Sci.*, 2016, **7**, 1620.
8 R. Pude, C. H. Treseler and G. Noga, *J. Appl. Bot.*, 2004, **78**, 58.
9 R. Pude, C. H. Treseler, R. Trettin and G. Noga, *Die Bodenkultur*, 2005, **56**, 61.
10 E. A. Heaton, F. G. Dohleman and A. Fernando Miguez, *et al.* *Miscanthus*: A Promising Biomass Crop, *Advances in Botanical Research*, Elsevier, 2010, vol. 56, pp. 0065–2296/10.
11 C. Emmerling and R. Pude, *GCB Bioenergy*, 2017, **9**, 274.
12 N. Brosse, A. Dufour, X. Meng, Q. Sun and A. Ragauskas, *Biofuels, Bioprod. Biorefin.*, 2012, **6**, 580.
13 S. Scagline-Mellor, T. Griggs, J. Skousen, E. Wolfrum and I. Holásková, *BioEnergy Res.*, 2018, **11**, 562.
14 I. Hafez and E. B. Hassan, *Energy Convers. Manage.*, 2015, **91**, 219.
15 T. Kraska, B. Kleinschmidt, J. Weinand and R. Pude, *Sci. Hortic.*, 2018, **235**, 205.
16 W. Schutyser, T. Renders, S. Van den Bosch, S. F. Koelewijn, G. T. Beckham and B. F. Sels, *Chem. Soc. Rev.*, 2018, **47**, 852.
17 M. N. Collins, M. Nechifor, F. Tanasă, M. Zănoagă, A. McLoughlin, M. A. Stróżyk, M. Culebras and C.-A. Teacă, *Int. J. Biol. Macromol.*, 2019, **131**, 828.
18 Z. Sun, B. Fridrich, A. de Santi, S. Elangovan and K. Barta, *Chem. Rev.*, 2018, **118**, 614.
19 Z. Jia, C. Lu, P. Zhou and L. Wang, *RSC Adv.*, 2015, **5**, 53949–53955.
20 G. Griffini, V. Passoni, R. Suriano, M. Levi and S. Turri, *ACS Sustainable Chem. Eng.*, 2015, **3**, 1145–1154.
21 S. E. Klein, J. Rumpf, P. Kusch, R. Albach, M. Rehahn, S. Witzleben and M. Schulze, *RSC Adv.*, 2018, **8**, 40765.
22 S. E. Klein, J. Rumpf, M. Rehahn, S. Witzleben and M. Schulze, *J. Coat. Technol. Res.*, 2019, **16**, 1543.
23 S. E. Klein, A. Alzagameem, J. Rumpf, I. Korte, J. Kreyenschmidt and M. Schulze, *Coatings*, 2019, **9**, 494.
24 T. Van der Weijde, A. Kiesel, Y. Iqbal, H. Muylle, O. Dolstra, R. G. F. Visser, I. Lewandowski and L. M. Trindade, *GCB Bioenergy*, 2016, **9**, 176.
25 Y. A. Gismatulina and V. V. Budaeva, *Ind. Crops Prod.*, 2017, **109**, 227.
26 Y. Iqbal and I. Lewandowski, *Fuel Process. Technol.*, 2014, **121**, 47.
27 J. Schäfer, M. Sattler, Y. Iqbal, I. Lewandowski and M. Bunzel, *GCB Bioenergy*, 2019, **11**, 191.
28 R. M. F. da Costa, S. J. Lee, G. G. Allison, S. P. Hazen, A. Winters and M. Bosch, *Ann. Bot.*, 2014, **114**, 1265.
29 R. M. F. da Costa, S. Pattathil, U. Avci, *et al.*, *Biotechnol. Biofuels*, 2019, **12**, 85.
30 A. Tolbert, H. Akinosho, R. Khunsupat, A. K. Naskar and A. J. Ragauskas, *Biofuels, Bioprod. Biorefin.*, 2014, **8**, 836.
31 R. El Hage, N. Brosse, L. Chrusciel, C. Sanchez, P. Sannigrahi and A. Ragauskas, *Polym. Degrad. Stab.*, 2009, **94**, 1632.
32 R. El Hage, N. Brosse, P. Sannigrahi and A. Ragauskas, *Polym. Degrad. Stab.*, 2010, **95**, 997.
33 R. El Hage, D. Perrin and N. Brosse, *Nat. Resour.*, 2012, **3**, 29.
34 S. Bauer, H. Sorek, V. D. Mitchell, A. B. Ibáñez and D. E. Wemmer, *J. Agric. Food Chem.*, 2012, **60**, 8203.
35 K. Wang, S. Bauer and R. Sun, *J. Agric. Food Chem.*, 2012, **60**, 144.
36 J. M. W. Chan, S. Bauer, H. Sorek, S. Sreekumar, K. Wang and F. D. Toste, *ACS Catal.*, 2013, **3**, 1369.
37 H. Luo, I. M. Klein, Y. Jiang, H. Zhu, B. Liu, H. I. Kenttämaa and M. M. Abu-Omar, *ACS Sustainable Chem. Eng.*, 2016, **4**, 2316.
38 A. Sorensen, P. J. Teller, T. Hilstrøm and B. K. Ahring, *Bioresour. Technol.*, 2008, **99**, 6602.
39 P. W. Baker, A. Winters and M. D. C. Hale, *BioResources*, 2016, **11**, 4379.
40 A. M. Sonnenberg, J. J. P. Baars, M. H. M. Visser, B. Lavrijssen and P. M. Hendrickx, *TKI T&U: KV 1310-032*, PPO/PRI report 2016-3, 2016, DOI: 10.18174/401882.
41 Y.-L. Cha, G. H. An, J. Yang, Y.-H. Moon, G.-D. Yu and J.-W. Ahn, *Renewable Energy*, 2015, **80**, 259.
42 Y. P. Timilsena, C. J. Abeywickrama, S. K. Rakshit and N. Brosse, *Bioresour. Technol.*, 2013, **135**, 82.
43 J. J. Villaverde, J. Li, M. Ek, P. Ligero and A. Vega, *J. Agric. Food Chem.*, 2009, **57**, 6262.
44 J. J. Villaverde, P. Ligero and A. Vega, *Open Agric. J.*, 2010, **4**, 102.
45 C. Vanderghem, A. Richel, N. Jacquet, C. Blecker and M. Paquot, *Polym. Degrad. Stab.*, 2011, **96**, 1761.
46 F. J. V. Gschwend, F. Malaret, S. Shinde, A. Brandt-Talbot and J. P. Hallett, *Green Chem.*, 2018, **20**, 3486.
47 A. Brandt, L. Chen, B. E. van Dongen, T. Welton and J. P. Hallett, *Green Chem.*, 2015, **17**, 5019.

Open Access Article. Published on 13 March 2020. Downloaded on 8/8/2024 5:01:17 AM.
This article is licensed under a Creative Commons Attribution-NonCommercial 3.0 Unported Licence.

48 G. S. Groenewold, K. M. Johnson, S. C. Fox, C. Rae, C. A. Zarzana, B. R. Kersten, S. M. Rowe, T. L. Westover, G. L. Gresham and R. M. Emerson, *Energy Fuels*, 2017, **31**, 1620.
49 J. Vasco-Correra and Y. Li, *Bioresour. Technol.*, 2015, **185**, 211.
50 R. Wahid, S. Frydendal Nielsen, V. Moset Hernandez, A. J. Ward, R. Gislum, U. Jørgensen and H. B. Møller, *Biosyst. Eng.*, 2015, **133**, 71.
51 N. Amougou, I. Bertrand, J.-M. Machet and S. Recous, *Plant Soil*, 2011, **338**, 83.
52 M. Battaglia, J. Fike, W. Fike, A. Sadeghpour and A. Diatta, *Grassl. Sci.*, 2019, **65**, 233.
53 T. Le Ngoc Huyen, C. Rémond, R. M. Dheilly and B. Chabbert, *Bioresour. Technol.*, 2010, **101**, 8224.
54 *Miscanthus nagara*, Available online: www.tinplant-gmbh.de accessed on October 18, 2019.
55 M. Deuter, *Miscanthus* Plant Named "MBS 7001", US Plant Patent PP22,033 P2, July 19, 2011.
56 E. A. Heaton, F. G. Dohleman, A. F. Miguez, J. A. Juvik, V. Lozovaya, J. Widholm and S. P. Long, *Adv. Bot. Res.*, 2010, **56**, 76.
57 P. C. Friesen, M. M. Peixoto, F. A. Busch, D. C. Johnson and R. F. Sage, *J. Exp. Bot.*, 2014, **65**, 3749.
58 M. de Melo Peixoto, P. C. Friesen and R. F. Sage, *J. Exp. Bot.*, 2015, **66**, 4415.
59 L. L. Smith, D. J. Allen and J. N. Barney, *Biomass Bioenergy*, 2015, **73**, 145–154.
60 H. Dong, S. V. Green, A. Nishiwaki, T. Yamada, J. R. Stewart, M. Deuter and E. J. Sacks, *GCB Bioenergy*, 2019, **11**, 691.
61 M. Bergs, G. Völkering, T. Kraska, X.-T. Do, Y. Monakhova, C. Konow, R. Pude and M. Schulze, *Int. J. Mol. Sci.*, 2019, **20**, 1200.
62 P. Obama, G. Ricochon, L. Muniglia and N. Brosse, *Bioresour. Technol.*, 2012, **112**, 156.
63 R. J. H. Grisel, J. C. van der Waal, E. de Jong and W. J. J. Huijgen, *Catal. Today*, 2014, **223**, 3.
64 A. Toledano, L. Serrano and J. Labidi, *Fuel*, 2014, **116**, 617.
65 *Determination of Structural Carbohydrates and Lignin in Biomass*, Available online: https://www.nrel.gov/docs/gen/fy13/42618.pdf, accessed on October 18, 2018.
66 A. Sluiter, B. Hames, R. Ruiz, C. Scarlata, J. Sluiter, D. Templeton and D. Crocker, *Determination of structural carbohydrates and lignin in biomass*, Laboratory analytical procedure, 2008, p. 1617.
67 A. Sluiter, R. Ruiz, C. Scarlata, J. Sluiter and D. Templeton, *Determination of extractives in biomass*, NREL/TP-510-42619, National Renewable Energy Laboratory, Golden, 2008.
68 A. Sluiter, B. Hames, D. Hyman, C. Payne, R. Ruiz, C. Scarlata, J. Sluiter, D. Templeton and J. Wolfe, *Determination of total solids in biomass and total dissolved solids in liquid process samples*, NREL Technical Report No. NREL/TP-510-42621 2008, National Renewable Energy Laboratory, Golden, CO, pp. 1–6.
69 A. Sluiter, B. Hames, R. Ruiz, C. Scarlata, J. Sluiter and D. Templeton, *Determination of ash in biomass*, NREL/TP-510-42622, National Renewable Energy Laboratory, Golden 2005.
70 A. Lourenço, J. Gominho and H. Pereira, Chemical characterization of lignocellulosic materials by analytical pyrolysis, in *Analytical Pyrolysis*, ed. P. Kusch, IntechOpen, London, UK, 1st edn, November 5th 2018, DOI: 10.5772/intechopen.80556.
71 C. G. Boeriu, F. I. Fitigau, R. J. A. Gosselink, A. E. Frissen, J. Stoutjesdijk and F. Peter, *Ind. Crops Prod.*, 2014, **62**, 481.
72 C. S. Lancefield, S. Constant, P. de Peinder and P. C. A. Bruijnincx, *ChemSusChem*, 2019, **12**, 1139.
73 R. A. Lee, C. Bédard, V. Berberi, R. Beauchet and J.-M. Lavoie, *Bioresour. Technol.*, 2013, **144**, 658.
74 D. Ahuja, A. Kaushik and G. S. Chauhan, *Int. J. Biol. Macromol.*, 2017, **97**, 403.
75 A. Alzagameem, B. El Khaldi-Hansen, D. Büchner, M. Larkins, B. Kamm, S. Witzleben and M. Schulze, *Molecules*, 2018, **23**, 2664.
76 P. Azadi, O. R. Inderwildi, R. Farnood and D.-A. King, *Renewable Sustainable Energy Rev.*, 2013, **21**, 506.
77 V. Vivekand, A. Chawade, M. Larsson, A. Larsson and O. Olsson, *Ind. Crops Prod.*, 2014, **59**, 1.
78 M. Norambuena, C. Vidal, L. Carrasco, D. Contreras and R. T. Mendonça, *Alkaline-catalyzed Modification of Organosolv Lignin: Optimization of Experimental Conditions. 5rd Nordic Wood Biorefinery Conference (NWBC 2015)*, Helsinki, Finland.
79 C. Domínguez, M. Oliet, M. A. Gilarranz and F. Rodríguez, *Ind. Crops Prod.*, 2008, **27**, 150.
80 E. M. Hodgson, D. J. Nowakowski, I. Shield, A. Riche, A. V. Bridgwater, J. C. Clifton-Brown and I. S. Donnison, *Bioresour. Technol.*, 2011, **102**, 3411.
81 B. Hansen, P. Kusch, M. Schulze and B. Kamm, *J. Polym. Environ.*, 2016, **24**, 85.
82 J. S. Lupoi, S. Singh, R. Parthasarathi, B. A. Simmons and R. J. Henry, *Renewable Sustainable Energy Rev.*, 2015, **49**, 871.
83 R. Vanholme, B. Demedts, K. Morreel, J. Ralph and W. Boerjan, *Plant Physiol.*, 2010, **153**, 895.
84 J. Ralph, C. Lapierre and W. Boerjan, *Curr. Opin. Biotechnol.*, 2019, **56**, 240.
85 J. R. D. Montgomery, C. S. Lancefield, D. M. Miles-Barrett, K. Ackermann, B. E. Bode, N. J. Westwood and T. Lebl, *ACS Omega*, 2017, **2**, 8466.
86 T. Ohraaho and J. Linnekoski, *J. Anal. Appl. Pyrolysis*, 2015, **113**, 186.
87 S. Wang, B. Ru, H. Lin, W. Sun and Z. Luo, *Bioresour. Technol.*, 2015, **182**, 120.
88 S. Wang, G. Dai, H. Yang and Z. Luo, *Prog. Energy Combust. Sci.*, 2017, **62**, 33.
89 H. Yang, R. Yan, H. Chen, D. H. Lee and C. Zheng, *Fuel*, 2007, **86**, 1781.
90 X. Du, M. Pérez-Boada, C. Fernández, J. Rencoret, J. C. del Río, J. Jiménez-Barbero, J. Li, A. Gutiérrez and A. T. Martínez, *Planta*, 2014, **239**, 1079.
91 X. Meng, A. Parikh, B. Seemala, R. Kumar, Y. Pu, P. Christopher, C. E. Wyman, C. M. Cai and A. J. Ragauskas, *ACS Sustainable Chem. Eng.*, 2018, **6**, 8711.
92 K. Cheng, H. Sorek, H. Zimmermann, D. E. Wemmer and M. Pauly, *Anal. Chem.*, 2013, **85**, 3213.

 This journal is © The Royal Society of Chemistry 2020

Open Access Article. Published on 13 March 2020. Downloaded on 8/8/2024 5:01:17 AM.
This article is licensed under a Creative Commons Attribution-NonCommercial 3.0 Unported Licence.

93 X. Li, Y. Wei, J. Xu, N. Xu and Y. He, *Biofuels*, 2018, **11**, 263.
94 M. N. Uddin, J. Nayeem, M. S. Islam and M. S. Jahan, *Biomass Convers. Biorefin.*, 2019, **9**, 35.
95 C. J. G. Colares, T. C. M. Pastore, V. T. R. Coradin, J. A. A. Camargos, A. C. O. Moreira, J. C. Rubimb and J. W. B. Braga, *J. Braz. Chem. Soc.*, 2015, 1–10, DOI: 10.5935/0103-5053.20150096.
96 L. M. Aguilera-Saeza, F. M. Arrabal-Camposa, A. J. Callejon-Ferreb, M. D. Suarez Medina and I. Fernandez, *Phytochemistry*, 2019, **158**, 110.
97 M. Mancini, D. Duca and G. Toscano, *J. Near Infrared Spectrosc.*, 2019, 1–11.
98 C. Christou, A. Agapiou and R. Kokkinofta, *J. Adv. Res.*, 2018, **10**, 1.
99 R. J. A. Gosselink, J. E. G. van Dam, E. de Jong, E. L. Scott, J. P. M. Sanders, J. Li and G. Gellerstedt, *Holzforschung*, 2010, **64**, 193.